

INVESTIGATION OF FORCED TORSIONAL VIBRATION MODES OF AN ATOMIC FORCE MICROSCOPY AND EFFECTS OF GEOMETRICAL PARAMETERS ON THE RESONANT FREQUENCY

SAJJAD YAZDANI^a, SAJJAD BIGHAM^a, JAVAD YAZDANI^b

^a*School of Mechanical Engineering, University of Tehran, Tehran, Iran*

^b*Nanoscience and Nanotechnology Research Center, Razi University, Kermanshah, 67149, Iran*

The torsional vibration modes of an Atomic Force Microscopy (AFM) cantilever with a sidewall probe and an AFM cantilever without a sidewall probe, When the AFM is scanning a sinusoidal shape sample surface is analyzed. Also In order to better design of an AFM, effect of geometrical parameter such as the cantilever length, cross section width of the cantilever probe thickness, cross section width, and tip length of the AFM without side and sidewall length of the AFM with sidewall on the resonant frequency is investigated.

(Received January 2, 2009; accepted January 6, 2009)

Keywords: AFM, torsional vibration, resonant frequency

1. Introduction

Atomic Force Microscopy (AFM) systems are powerful and useful technique in nanoscale science and technologies such as surface science and biomaterials. AFM has been widely developed as an effective tool for obtaining atomic-scale images and the material surface properties [1-8] AFM has widely applications in various sciences. Some of these applications are nanolithography in MEMS-NEMS (Micro-Nano Electro-Mechanical Systems) [9-11] and surface characterization in material science, to the study of living biological systems in their natural environment, to nanolithography and topographical analysis of soft materials such as DNA and lubricant molecule, also AFM provides chance to study particles without fixing, in aqueous environment.

In AFM systems, a sharp probe at the end of a cantilever interacting locally with the sample surface is scanned by a piezoelectric scanner, providing three-dimensional information about the surface. It is well known that a customary cantilever with a tip at the free end plays an important role in AFM measurements.

When a tip scans across a sample surface, it induces a dynamic interaction force between the tip and the surface. Dynamic responses of the AFM cantilever has been investigated by many researches [12-18]

Some of researchers [19-24] have been studied the vibration response of an AFM cantilever for convenience without considering the interactive damping Turner et al. [25] and Rabe et al. [26], have been shown the effect of damping on the vibration response of an AFM cantilever is very important.

*Corresponding author: s.bigham @me.ut.ac.ir

Effect of interactive damping on sensitivity of vibration modes of rectangular AFM cantilevers has been investigated by Chang et al. [27]. Long Lee and Chang [28] have been studied Coupled lateral bending and torsional vibration sensitivity of atomic force microscope cantilever. More recently Yazdani et al. [29] investigated the analytical solution of interactive damping and longitudinal and normal contact stiffness on sensitivity of vibration modes of rectangular AFM cantilevers. Chang et al. [30] studied the sensitivity of the first four flexural modes of an AFM cantilever with a sidewall probe. Their results showed that a sidewall scanning AFM is more sensitive when the contact stiffness is lower and that the first mode is the most sensitive. Also they found the resonance frequency of an AFM cantilever is low when contact stiffness is small, however, the frequency rapidly increases as contact stiffness increases.

The objective of the current study is to investigate sensitivity of the torsional modes of an AFM cantilever with a sidewall probe and AFM cantilever without sidewall probe and study effect of sidewall on the torsional modal sensitivity as the contact surface is modeled with *sin* shape sample surface.

2. Analysis

Figure (1) shows the schematic of sinusoidal shape sample surface. When an AFM is scanning a sinusoidal shape sample surface, the forces induced to AFM are function of $\sin(\omega t)$, where ω is the angular frequency of these forces. Effect of these forces can be modeled by a sinusoidal torsional couple.

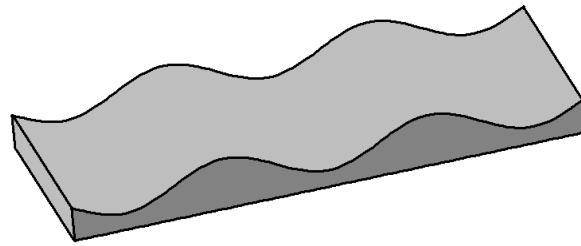


Fig.1. Schematic of a *sin* shape sample surface

Figure (2.a) shows the schematic of an AFM without sidewall and Figure (2.b) shows the schematic of an AFM with sidewall. Both AFM have uniform cross section thickness a , width b , length L for horizontal cantilever and length, tip length h of the AFM without sidewall and vertical extension length h of the AFM with sidewall. An AFM with sidewall has a horizontal cantilever and a vertical extension at the free end, and a tip located at the free end of the vertical extension is able to probe in a direction perpendicular to sidewall. The probe named as ‘‘Assembled Cantilever Probe’’.

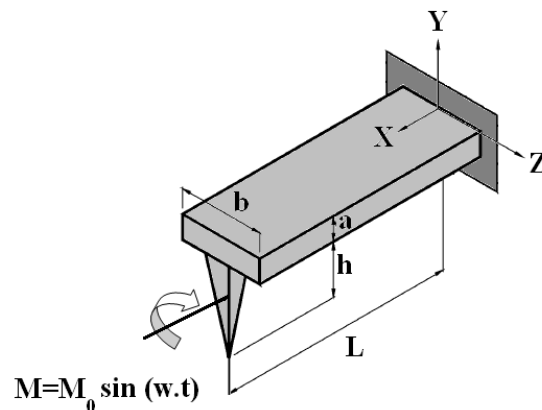


Fig.2.a. Schematic diagram of an AFM cantilever without sidewall.

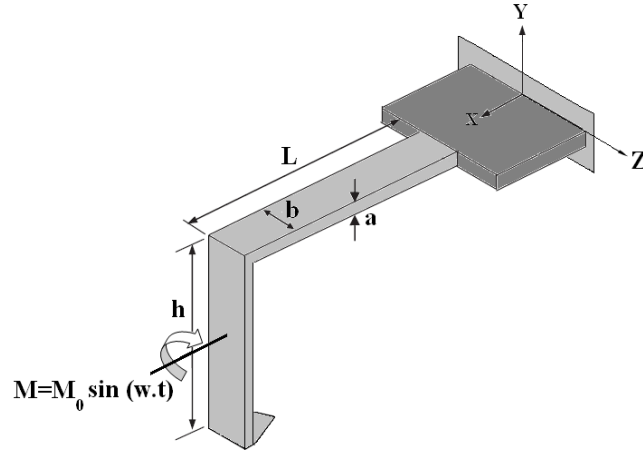


Fig.2.b. Schematic diagram of an AFM cantilever micro assembled with a vertical extension at the free end and a tip located at the free end of the vertical extension.

The linear differential equation of motion for the torsional vibration of the cantilever can be expressed as [31, 32]

$$G\eta \frac{\partial^2 \theta(x,t)}{\partial x^2} = \rho I_p \frac{\partial^2 \theta(x,t)}{\partial t^2} \quad (1)$$

where θ is the angle of torsion of the cross-sectional area shown in Fig. 1, G is the modulus of shear, I_p is the polar moment of area, η is the torsional parameter

$$\eta = \frac{1}{3} ab^3 \left(1 - 0.63 \frac{a}{b}\right) \quad (2)$$

The boundary conditions are

$$\theta(0,t) = 0 \quad (3)$$

$$M_0 - G\eta \frac{\partial \theta(L,t)}{\partial x} = -J_0 \frac{\partial^2 \theta(L,t)}{\partial t^2} \quad (4)$$

where J_0 is moment of inertia of the vertical extension. Eq. (3) is the condition of the cantilever beam end being fixed, and Eq. (4) is the couple balance at $x = L$. A general solution of Eq. (1), with boundary condition (3) and (4) can be expressed as:

$$\theta(x,t) = \psi(x) \sin(\omega t) \quad (5)$$

where ω is the angular frequency. Substituting Eq. (5) into Eq. (1)

$$\psi(x) = A \sin\left(\sqrt{\frac{\rho I_p}{G\eta}} x\right) + B \cos\left(\sqrt{\frac{\rho I_p}{G\eta}} x\right) \quad (6)$$

Where A and B, are constants determined from the boundary conditions. Substituting Eq. (6) into Eq. (3)

$$B = 0 \quad (7)$$

Substituting Eq. (6) into Eq (4):

$$A = \frac{M_0}{[\eta G \sqrt{\frac{\rho I_p}{G \eta}} \omega \cos(\sqrt{\frac{\rho I_p}{G \eta}} L \omega) - J_0 \omega^2 \sin(\sqrt{\frac{\rho I_p}{G \eta}} L \omega)]} \quad (8)$$

Substituting Eq. (6, 7, 8) into Eq(5):

$$\theta(x,t) = \frac{M_0}{GI_p} \left\{ \frac{\sin(\sqrt{\frac{\rho I_p}{G \eta}} \omega x)}{[\sqrt{\frac{\rho I_p}{G \eta}} L \omega \cos(\sqrt{\frac{\rho I_p}{G \eta}} L \omega) - \frac{J_0 L \omega^2}{I_p G} \sin(\sqrt{\frac{\rho I_p}{G \eta}} L \omega)]} \right\} \sin \omega t \quad (9)$$

In order to determine natural frequency of the system by setting $M_0=0$ into Eq (4) and solve Eq (1) again:

$$\omega_n \tan\left(L \sqrt{\frac{\rho I_p}{G \eta}} \omega_n\right) = \frac{\sqrt{G \eta \rho I_p}}{J_0} \quad (12)$$

It is obviously that as $\omega = (\omega_n)_{\text{system}}$ phenomenon of resonance will occur. The relation between ω and f where f is frequency is given by

$$f = \frac{1}{2\pi} \omega \quad (12)$$

By substituting Eq. (13) into Eq(12):resonance frequency is obtained by

$$f_{\text{Res}} \tan\left(2\pi L \sqrt{\frac{\rho I_p}{G \eta}} f_{\text{Res}}\right) = \frac{\sqrt{G \eta \rho I_p}}{2\pi J_0} \quad (10)$$

Where f_{Res} is resonant frequency.

3. Results and discussions

The torsional vibration modes of an AFM cantilever with a sidewall probe and an AFM cantilever without a sidewall probe, When the AFM is scanning a sinusoidal shape sample surface is investigated. In order to know the effect of relative parameters on the sensitivity and resonant frequency, we considered the geometric and material parameters as follows: $G=66.4$ GPa, $\rho=2330$

kg/m³, L=300 μ m, a=2 μ m, b=50 μ m, h=10 μ m for the AFM cantilever without sidewall and h=150 μ m for the AFM cantilever with a sidewall probe. In order to better design of an AFM, effects of geometrical parameter on the resonant frequency are investigated. As the effect of a specific geometrical parameter is investigated the other geometrical parameters are constant at above reference values. Resonant frequencies of mode 1 to mode 6 at various values of cantilever lengths are listed in table 1 for an AFM without sidewall and table 2 for an AFM with sidewall. It is seen as the cantilever length increases, resonant frequencies decreases at all modes for both AFM.

Table 1. Resonant frequency of modes (1-6) at b=50 μ m, a=2 μ m and h=10 μ m for an AFM without sidewall.

L=100 μm	L=200 μm	L=300 μm
1021343.85000000	518402.250000000	347358.450000000
1052759.85000000	526378.650000000	350918.250000000
3064561.95000000	1555242.45000000	1042075.35000000
3158279.55000000	1579141.05000000	1052759.85000000
5109320.25000000	2592189.75000000	1736817.75000000
5263799.25000000	2631898.35000000	1754601.45000000

Table 2. Resonant frequency of modes (1-6) at b=50 μ m, a=2 μ m and h=150 μ m for an AFM with sidewall.

L=100 μm	L=200 μm	L=300 μm
88905.750000000	62681.550000000	51028.050000000
1052759.85000000	526378.650000000	350918.250000000
2109291.15000000	1056523.65000000	705597.750000000
3158279.55000000	1579141.05000000	1052759.85000000
4212928.95000000	2107404.15000000	1405567.65000000
5263799.25000000	2631898.35000000	1754601.45000000

Resonant frequencies of mode 1 to mode 6 at various values of cross section widths of the cantilever probe thickness are given in table 3 for an AFM without sidewall and table 4 for an AFM with sidewall. It can be found as cross section width of the cantilever probe thickness increases, resonant frequencies increases at all modes for both AFM.

Table 3. Resonant frequency of modes (1-6) at L=300 μ m, b=50 μ m, and h=10 μ m for an AFM without sidewall.

a=0.6 μm	a=2 μm	a=7 μm
105266.550000000	347358.450000000	1163067.75000000
106301.850000000	350918.250000000	1177337.55000000
315804.750000000	1042075.35000000	3489244.05000000
318905.550000000	1052759.85000000	3532007.55000000
526342.950000000	1736817.75000000	5815547.85000000
531509.250000000	1754601.45000000	5886682.65000000

Table 4. Resonant frequency of modes (1-6) at $L=300 \mu\text{m}$, $b=50 \mu\text{m}$, and $h=150 \mu\text{m}$ for an AFM with sidewall.

a=0.6 μm	a=2 μm	a=7 μm
15552.4500000000	51028.0500000000	168679.9500000000
106301.8500000000	350918.2500000000	1177337.5500000000
213753.7500000000	705597.7500000000	2366902.3500000000
318905.5500000000	1052759.8500000000	3532007.5500000000
425786.2500000000	1405567.6500000000	4715482.9500000000
531509.2500000000	1754601.4500000000	5886682.6500000000

Resonant frequencies of mode 1 to mode 6 at various values cross section widths are listed in table 5 for an AFM without sidewall and table 6 for an AFM with sidewall. It is seen as cross section widths of the cantilever increases, resonant frequencies decreases at all modes for both AFM except first mode of AFM with sidewall width: $b=50 \mu\text{m}$.

Table 5. Resonant frequency of modes (1-6) at $L=300 \mu\text{m}$, $a=2 \mu\text{m}$, and $h=10 \mu\text{m}$ for an AFM without sidewall.

b=20 μm	b=50 μm	b=70 μm
839518.6500000000	347358.4500000000	249356.8500000000
856537.3500000000	350918.2500000000	251677.3500000000
2518683.4500000000	1042075.3500000000	748075.6500000000
2569612.0500000000	1052759.8500000000	755037.1500000000
4198230.7500000000	1736817.7500000000	1246799.5500000000
4282691.8500000000	1754601.4500000000	1258396.9500000000

Table 6. Resonant frequency of modes (1-6) at $L=300 \mu\text{m}$, $a=2 \mu\text{m}$, and $h=150 \mu\text{m}$ for an AFM with sidewall.

b=20 μm	b=50 μm	b=70 μm
50966.8500000000	51028.0500000000	50176.3500000000
856537.3500000000	350918.2500000000	251677.3500000000
1714597.0500000000	705597.7500000000	508477.6500000000
2569612.0500000000	1052759.8500000000	755037.1500000000
3426911.8500000000	1405567.6500000000	1009297.6500000000
4282691.8500000000	1754601.4500000000	1258396.9500000000

Resonant frequencies of mode 1 to mode 6 at various values of tip lengths are given in table 7 for an AFM without sidewall and resonant frequencies of mode 1 to mode 6 at various values of sidewall lengths are given in table 8 for an AFM with sidewall. It is found that as the tip lengths increases, resonant frequencies decreases at all modes for the AFM without sidewall also as the sidewall length increases, resonant frequencies decreases at all modes for the AFM with sidewall.

Table 7. Resonant frequency of modes (1-6) at $L=300 \mu\text{m}$, $a=2 \mu\text{m}$, and $b=50 \mu\text{m}$ for an AFM without sidewall.

h=5 μm	h=10 μm	h=20 μm
349347.450000000	347358.450000000	340850.850000000
350918.250000000	350918.250000000	350918.250000000
1048047.450000000	1042075.350000000	1022710.650000000
1052759.850000000	1052759.850000000	1052759.850000000
1746742.350000000	1736817.750000000	1705029.450000000
1754601.450000000	1754601.450000000	1754601.450000000

Table 8. Resonant frequency of modes (1-6) at $L=300 \mu\text{m}$, $a=2 \mu\text{m}$, and $b=50 \mu\text{m}$ for an AFM with sidewall.

h=50 μm	h=100 μm	h=150 μm
201784.050000000	90043.050000000	51028.050000000
350918.250000000	350918.250000000	350918.250000000
773259.450000000	713844.450000000	705597.750000000
1052759.850000000	1052759.850000000	1052759.850000000
1442904.750000000	1409764.950000000	1405567.650000000
1754601.450000000	1754601.450000000	1754601.450000000

4. Conclusion

The torsional vibration modes of an AFM cantilever with a sidewall probe and an AFM cantilever without a sidewall probe, When the AFM is scanning a sinusoidal shape sample surface has been analyzed. Results showed as the cantilever length increases, resonant frequencies decreases and resonant frequencies increases as cross section width of the cantilever probe thickness increases at all modes for both AFM. It was found as cross section width of the cantilever increases, resonant frequencies decreases at all modes for both AFM except first mode of AFM with sidewall with $b=50 \mu\text{m}$. Resonant frequencies decreases when the tip length increases for the AFM without sidewall also as the sidewall length increases, resonant frequencies decreases at all modes for the AFM with sidewall.

References

- [1] K. Holmberg, A. Matthews, Coatings Tribology: Properties, Techniques and Applications in Surface Engineering, Elsevier, New York, 1994.
- [2] P.E. Mazeran, J.L. Loubet, Tribol. Lett. **7**, 199 (1999).
- [3] B. Bhushan, Handbook of Micro/Nanotribology, second ed., CRC, Boca Raton, FL, 1999.
- [4] Giessibl F. J., "Advances in Atomic Force Microscopy," Reviews of Modern Physics, **75**, 949 (2003).
- [5] Garcia R. and Perez R., "Dynamic atomic force microscopy methods," Surface Science Report, **47**, 197 (2002).
- [6] S. Lin, J.L. Chen, L.S. Huang, H.W. Lin, J. Curr. Proteomics **2**, 55 (2005).
- [7] R.J. Colton, J. Vac. Sci. Technol. B **22**, 1609 (2004).
- [8] N. Jalili, K. Laxminarayana, J. Mechatron. **14**, 907 (2004).
- [9] T. H. Fang, W. J. Chang, J. Phys. Chem. Solids **64**, 913 (2003).
- [10] W. J. Chang, T. H. Fang, C.I. Weng, Nanotechnology **15**, 427 (2004).
- [11] T. H. Fang, W. J. Chang, C. I. Weng, Mater. Sci. Eng. A **430**, 332 (2006).
- [12] O. Nakabeppu, M. Chandrachood, Y. Wu, J. Lai, A. Majumdar, Appl. Phys. Lett.

- 66**(6), 694 (1995).
- [13] U. Rabe, K. Janser, W. Arnold, *Rev. Sci. Instrum.* **67** (9), 3281 (1996).
 - [14] T. Drobek, R.W. Stark, M. Graber, W.M. Heckl, *New J. Phys.* **1**, 15.1 (1999).
 - [15] M. Ashhab, M.V. Salapaka, M. Dahleh, I. Mezic, *Automatica* **35**, 1663 (1999).
 - [16] O.B. Wright, N. Nishiguchi, *Appl. Phys. Lett.* **71** (5), 626 (1997).
 - [17] P.E. Mazeran, J.L. Loubet, *Tribology Lett.* **7**, 199 (1999).
 - [18] W. Weaver Jr., S.P. Timoshenko, D.H. Young, *Vibration Problems in Engineering*, fifth ed., Wiley, New York, 1990.
 - [19] S. Hirsekorn, U. Rabe, W. Arnold, *Nanotechnology* **8**, 57 (1997).
 - [20] K. Yamanaka, A. Noguchi, T. Tsuji, T. Koike, T. Goto, *Surf. Interface Anal.* **27**, 600 (1999).
 - [21] G.G. Yaralioglu, F.L. Degertekin, K.B. Crozier, C.F. Quate, *J. Appl. Phys.* **87** (10), 7491 (2000).
 - [22] R.F. Fung, S.C. Huang, *ASME J. Vibr. Acoust.* **123**, 502 (2001).
 - [23] R. Levy, M. Maaloum, *Nanotechnology* **13**, 33 (2002).
 - [24] H. Kawakatsu, S. Kawai, D. Saya, M. Nagashio, D. Kobayashi, H. Toshiyoshi, *Rev. Sci. Instrum.* **73**(6), 2317 (2002).
 - [25] J.A. Turner, S. Hirsekorn, U. Rabe, W. Arnold, *J. Appl. Phys.* **82**(3), 967 (1997).
 - [26] U. Rabe, J.A. Turner, W. Arnold, *Appl. Phys. A* **66**, S277 (1998).
 - [27] Win-Jin Chang, Te-Hua Fang, Huann-Ming Chou, *Physics Letters A* **312**, 158 (2003).
 - [28] Haw-Long Lee, Win-Jin Chang, *Ultramicroscopy* **108**, 707 (2008).
 - [29] J. Yazdani, S. Yazdani, S. Bigham, *Digest Journal of Nanomaterials and Biostructures*. **3**, 277 (2008).
 - [30] Win-Jin Chang, Haw-Long Lee, Terry Yuan-Fang Chen, *Ultramicroscopy* **108**, 619 (2008).
 - [31] W.J. Weaver, S.P. Timoshenko, D.H. Young, *Vibration Problems in Engineering*, 5th Edition, Wiley, New York, 1990.
 - [32] S. Timoshenko, J.N. Goodier, *Theory of Elasticity*, McGraw-Hill, New York, 1987.